Journal of Engineering and Technology Research Vol.1 (9), pp. 194-202, December, 2009
Available online at http://www.academicjournals.org/jetr
ISSN 2006-9790© 2009 Academic Journals

Full Length Research Paper

Turbulence study in the internal combustion engine

Z. Barbouchi* and J. Bessrour

Mechanics and industrialisation research unit (MA2I), Mechanical engineering department, National Engineering School of Tunis (E.N.I.T), B.P 37, 1002 Bélvédère Tunisia.

Accepted 13 November, 2009

In this paper, we are interested in the study of turbulent and time dependant flow inside a cylinder of an alternative engine through the investigation of the distribution of the turbulent kinetic energy in the whole space of the chamber. This research is carried out during the intake stroke. The arbitrary lagrangian eulerian technique coupled with the finite element method is used to solve the Navier Stokes equations. The turbulence model of the inlet air in the cylinder has a great influence in to the performance of the engine. It governs directly the rate of filling up, the thermal exchanges and the combustion quality. We present distribution of the velocity, pressure and turbulence field inside the engine room.

Key words: Turbulence, internal combustion engine, arbitrary lagrangian eulerian, tumble ratio, k-ε model, prandtl model, finite element method.

INTRODUCTION

In 1876, Nicolaus A. Otto developed the spark-ignition engine and in 1892 Rudolf Diesel invented the compression-ignition engine (Wei Li, 2000). They were the first who studied the internal combustion engines. The identification of the aerodynamic and thermal fields inside a cylinder of alternative engine with internal combustion during the intake stroke is an important stage for the comprehension of physical phenomenon which occurs in the motor cycle (Barbouchi and Bessrour 2008). Engine researches have attempted to maximize the power produced from fuel combustion. The piston speed, the piston chamber geometry, fuel composition, in-cylinder fluid dynamics and ignition devices used, represent the different variables that affect the internal combustion.

The aerodynamic phenomena which take place at the level of the valves have been studied often through the experiments. Many experimental essays have been carried out in the case of stationary flows to characterize the air movement through the valves (Arcoumanis et al., 1982; Kang and Reitz, 1999; Snauwaert and Sierens, 1986; Tippelmann, 1977) and recently (Gazeaux and Thomas, 2001; Yun J.E., 2002). It was established that the air flow through the valve interacts with the cylinder walls to create large swirling structures. Generally, the principal air movements were filed into categories: the rotary movement induced tangentially in the cylinder (swirl) and the rotary movement in the axial plane (tumble) (Heywood, 1987). It's clear that the flow generation with intense vorticity (swirl and/or tumble) in the cylinder during the intake stroke is an efficient tool to obtain a great intensity of turbulence which can be maintained during the compression stroke. The stability of these swirling movements allows so to maintain a large turbulence during the fuel injection phase and induce optimal conditions for the initiation and the development of the combustion process. The shape of the combustion chamber plays too an important role as for of the established flows (Barbouchi and Bessrour, 2008).

To study the turbulence, most models used in engineering practice employ the Boussinesq approximation, where the turbulent stresses in the Reynolds-averaged momentum and energy equations are assumed equal to the product of the isotropic eddy viscosity coefficients and the mean velocity strain rate. The eddy viscosity can be obtained by a direct dependence on the mean flow quantities, as in algebraic or zero-equation models. An auxiliary field equation or equations for the turbulent velocity and time scales can also be solved to obtain the eddy viscosity as in one- or two-equation models (Kral, 1998).

In this paper, we present a numerical simulation of

*Corresponding author. E-mail: zouhaierbarbouchi@yahoo.fr.

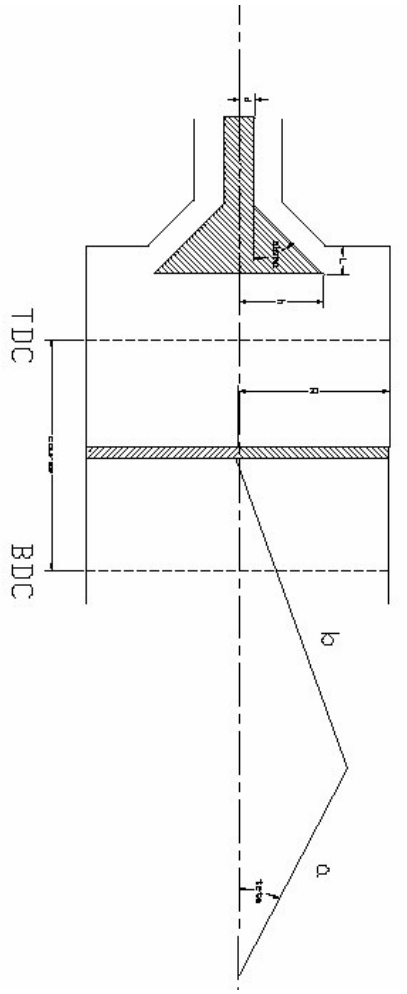

Figure 1. Axis-symmetrical piston cylinder.

aerodynamic field in axial plane of axis-symmetrical cylinder with axial valve and flat piston of internal combustion engine (Figure 1) in order to compare results with others coming from experiments and numerical predictions provided by literature. To take the variability of the domain into account and so the deformed mesh (Haworth and Jansen, 2000; Malcevic and Ghattas, 2002), we have tried to test the arbitrary Lagrangian Eulerian method (ALE) (Souli and Zolesio, 2001). We have developed numerical methodology based on finite element method by means of powerful calculation code (CASTEM of CEA) (Gounand, 1997).

R = 43.5 mm, h = 17 mm, d = 6.12 mm, α = 45°
S = 94 mm, L = 7.3 mm, a = S/2, b = 363.5 mm

MODELLING OF THE PROBLEM

The flow in the engine room is time dependant, incompressible and turbulent. The average equations describing the flow are:
Continuity equation:

$$\frac{\partial \rho}{\partial t} + div(\rho u) = 0 \quad (1)$$

Momentum equation:

$$\frac{\partial \rho.u}{\partial t} + div(\rho.u*u) = -\nabla P - \frac{2}{3}\nabla((\mu+\mu_t).\nabla u) + \nabla((\mu+\mu_t).(\nabla u + (\nabla u)^t)) \quad (2)$$

To solve the equations (1) and (2) we have to know the value of the turbulent viscosity μ_t. The concept of the turbulent viscosity was introduced by Boussinesq (1877). He supposes that the turbulent stresses in the Reynolds-averaged momentum equation are assumed equal to the product of the isotropic eddy viscosity coefficient and the mean velocity strain rate (Lee and Farrel, 1993).

$$R_{ij} = \mu_t \left(\frac{\partial U_i}{\partial x_j} + \frac{\partial U_j}{\partial x_i}\right) \quad (3)$$

With:
μ_t : Turbulent viscosity
R_{ij} : Reynolds tensor $R_{ij} = -\rho\overline{u_i' u_j'}$
$U_{i,j}$: velocity vector
u' : Favre averaged velocity
x: axial coordinate
y: normal coordinate

The concept of turbulence is based on taking each variable the sum of an averaged component and fluctuating component.

Reynolds's averaging method

The conventional method of Reynolds consists in breaking down each variable ϕ of the flow as described below:

$$\phi = \bar{\phi} + \phi' \quad (4)$$

With:

$$\bar{\phi} = \frac{1}{T}\int_{t_0}^{t_0+T} \phi\, dt \quad (5)$$

$\bar{\phi}$ is the time averaged component of the variable ϕ

ϕ' is the fluctuating component of the variable ϕ

Favre averaging method

This technique consists in decomposing the variable of the flow ϕ as following:

$$\phi = \tilde{\phi} + \phi'' \tag{6}$$

$\tilde{\phi}$ is the Favre averaged value of the variable ϕ defined by:

$$\tilde{\phi} = \frac{\overline{\rho\phi}}{\overline{\rho}} \tag{7}$$

Many turbulent models are proposed to understand the phenomenon of turbulence, since the k-ε model is frequently used in scientific researches, we have chosen with the Prandtl model to control turbulence.

k-ε model

The k-ε two-equation turbulence model is widely used in CFD applications today. The two equations models are called also completed models because, all the characteristics of turbulence, needed to specify the turbulent viscosity, are obtained from the transport equations. The k-ε model was proposed by Launder and Spalding (Launder and Spalding, 1974).

The turbulent kinetic energy is calculated as kinetic energy resulting of fluctuating velocities u', v', w'. Its mathematical expression is given by:

$$k = \frac{1}{2}\overline{u_i' u_i'} = \frac{1}{2}(\overline{u'^2} + \overline{v'^2} + \overline{w'^2})$$

In the sense of Reynolds (8)

$$k = \frac{1}{2}\frac{\overline{\rho u_i'' u_i''}}{\overline{\rho}} = \frac{1}{2}\frac{(\overline{\rho u''^2} + \overline{\rho v''^2} + \overline{\rho w''^2})}{\overline{\rho}}$$

In the sense of Favre (9)

We find, in this model, one equation for the turbulent kinetic energy k and another one for the turbulent energy dissipation rate ε.

$$\frac{\partial \rho k}{\partial t} + div(\rho . u . k) = div((\mu + \frac{\mu_t}{\sigma_k})\nabla k) + \rho . G - \rho\varepsilon \tag{10}$$

$$\frac{\partial \rho \varepsilon}{\partial t} + div(\rho . u . \varepsilon) = div((\mu + \frac{\mu_t}{\sigma_\varepsilon})\nabla \varepsilon) + C_{\varepsilon 1}\rho \frac{\varepsilon}{k} G - C_{\varepsilon 2}\rho \frac{\varepsilon^2}{k} \tag{11}$$

$$G = -\vec{u} * \vec{u} : \nabla \vec{u}$$
$$-\overline{\rho}\,\vec{u} * \vec{u} = \mu_t (\nabla \vec{u} + (\nabla \vec{u})) - \frac{2}{3}(\overline{\rho} k + \mu_t div \vec{u})\vec{\vec{I}} \tag{12}$$

The constants of the model derived from many experiments:

$$C_\mu = 0.09 \; ; \; C_1 = 1.44 \; ; \; C_2 = 1.92 \; ;$$
$$\sigma_\varepsilon = 1.3 \; ; \; \sigma_k = 0.9 \tag{13}$$

The turbulent viscosity is expressed according to the variables k and ε as below:

$$\mu_t = C_\mu \rho \frac{k^2}{\varepsilon} \tag{14}$$

Prandtl model

This model belongs to the algebraic (or zero-equation) models, where the turbulent viscosity is expressed according to the local variables of the average flow. It is directly linked to the average velocity fields and no transport equation is needed. Prandtl (Prandtl, 1925) proposed in 1925 the following formulation:

$$\mu_t = \rho l_m^2 \left|\frac{\partial U}{\partial y}\right| \tag{15}$$

ρ is the density. l_m is the characteristic length scale, depends generally on the coordinates and represents the scale of turbulence at a given point. Many empirical relations are used to calculate the parameter l_m. Among which we have chosen this expression:

$$l_m = R(0.14 - 0.08(1 - \frac{y}{R})^2 - 0.06(1 - \frac{y}{R})^4) \tag{16}$$

R: the radius of the combustion chamber

Boundary conditions

The boundary conditions adapted to the chosen configu-

ration (Figure 2) are listed below:

$$L1:\ v=0,\ L2:\ u=0;v=0$$

$$L3:\ u=V_p;v=0, L4:\ \frac{\partial u}{\partial n}=0;v=0 \quad (17)$$

u and v are respectively velocity components in axial direction and radial direction, V_p represents the piston speed.

RESULTS AND DISCUSSIONS

Firstly, before discussing the turbulence inside the combustion chamber, we have compared our numerical methodology with others coming from literature in order to validate our numerical simulation.

Validation of simulation

The finite element method is employed to solve the equations Navier Stokes system. Exactly, the Galerkin Proceeding is applied for spatial discretization. To solve the problem of the expansion of the mesh in time, we have included the arbitrary Lagrangian Eulerian method (ALE).

The Figure 3 shows three curves plotted when the crank angle θ is equal to 90°. The blue one is coming from experiments (Raghay and Hakim, 1997), the red curve is the result of Raghay and Hakim (1997) predictions and the yellow curve is obtained by our numerical simulation (Barbouchi and Bessrour, 2008). The simulation of Raghay and Hakim has employed the finite volume method and it represents the distribution of the velocity field all along the chamber radius and on the axial position x = 77 mm.

Compared to the Arcoumanis measurements these predictions present a large error. On the other hand, if we compare our numerical results with those experimental, we notice a good correspondence. Therefore, the finite element method with ALE description gives best results than the finite volume method.

Turbulent kinetic energy

To study the distribution of turbulent kinetic energy in the whole space of the combustion chamber, we have plot it according to the increasing of the radial coordinate which gives distance from the cylinder axis to the lateral wall. Too, we have changed the axial position and we have taken x = 27 mm, x = 52 mm and x = 77 mm Figure 4. All plots are taken for crank angle θ equal to 90°.

The Figure 4 shows that for the same step of time the intensity of the turbulent kinetic energy is maximum for

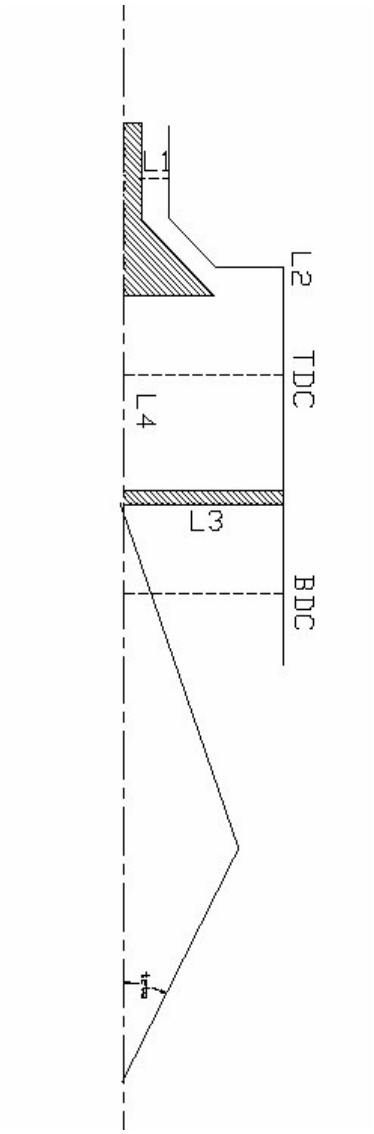

Figure 2. Intake phase configuration.

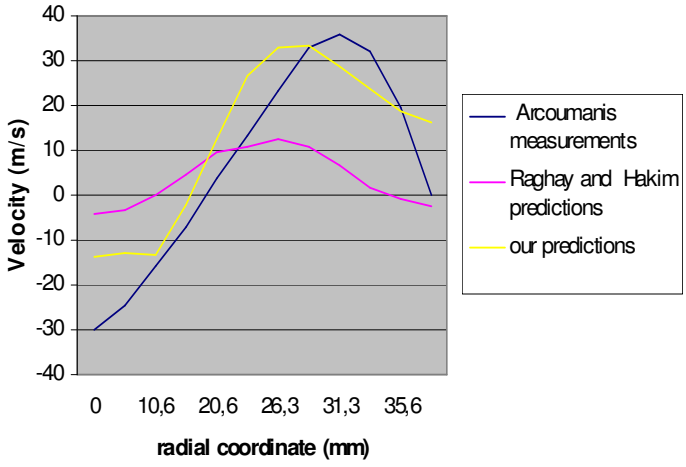

Figure 3. Velocity field comparison.

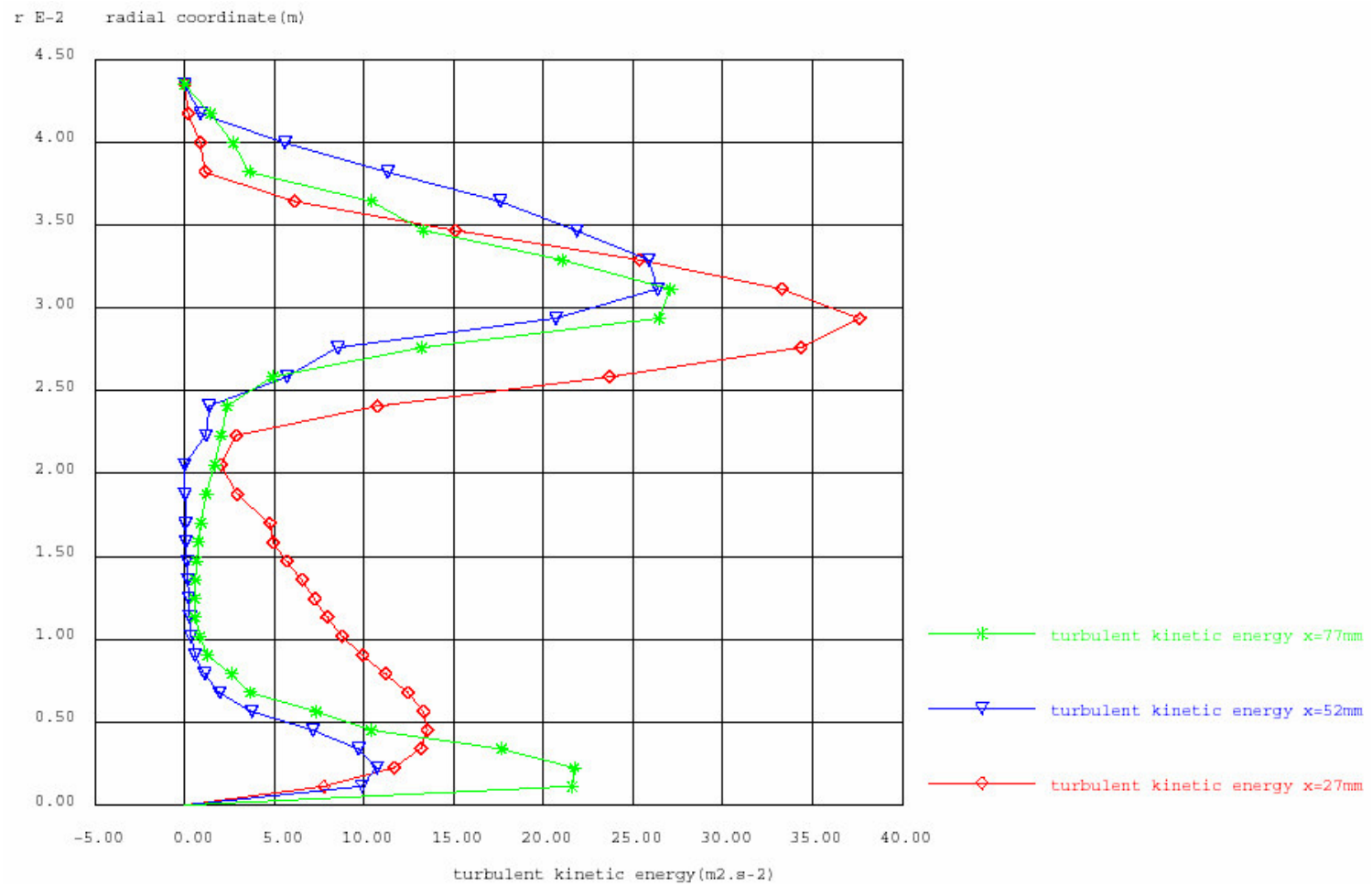

Figure 4. Turbulent kinetic energy for θ = 90°.

the axial position x = 27 mm. We can explain this by the fact that this region is near the air admission zone where the flow motion is disorganized. As well, for the three curves we notice that the peak of turbulence is obtained for radial coordinate r = 3 cm. Another smaller peak of turbulence appears near the cylinder axis.

The turbulent kinetic energy is drawn for θ = 180° (Figure 5). Then, for the three curves we can see that the intensity of turbulence becomes weak. Also, there is alternation between two peaks, the upper one and the lower one. The amplitude of turbulence is increasing from the cylinder lateral wall to the symmetry axis.

Tumble ratio

In order to quantify the turbulence more, a tumble ratio T_{ca} is calculated at each crank angle and plotted in Figure 6. This ratio is defined as follows:

$$T_{ca} = \frac{\sum_{i=1}^{n}\left(\frac{\partial v}{\partial x} - \frac{\partial u}{\partial y}\right)_i}{2n\omega} \quad (18)$$

Where $\left(\frac{\partial v}{\partial x} - \frac{\partial u}{\partial y}\right)$ is the vorticity for tumble ratio, the subscript i stands for the number of grids set up for the data points in the symmetry axial plane, n is the total number of grid points and ω the crank shaft angular speed in radians per second which can be calculated by $\omega = \frac{2\pi N}{60}$ (N is the engine speed in rpm). The numerator in equation (18) represents the total amount of large and small-scale rotations in the symmetry axial plane. The tumble ratio can be interpreted as the ratio of

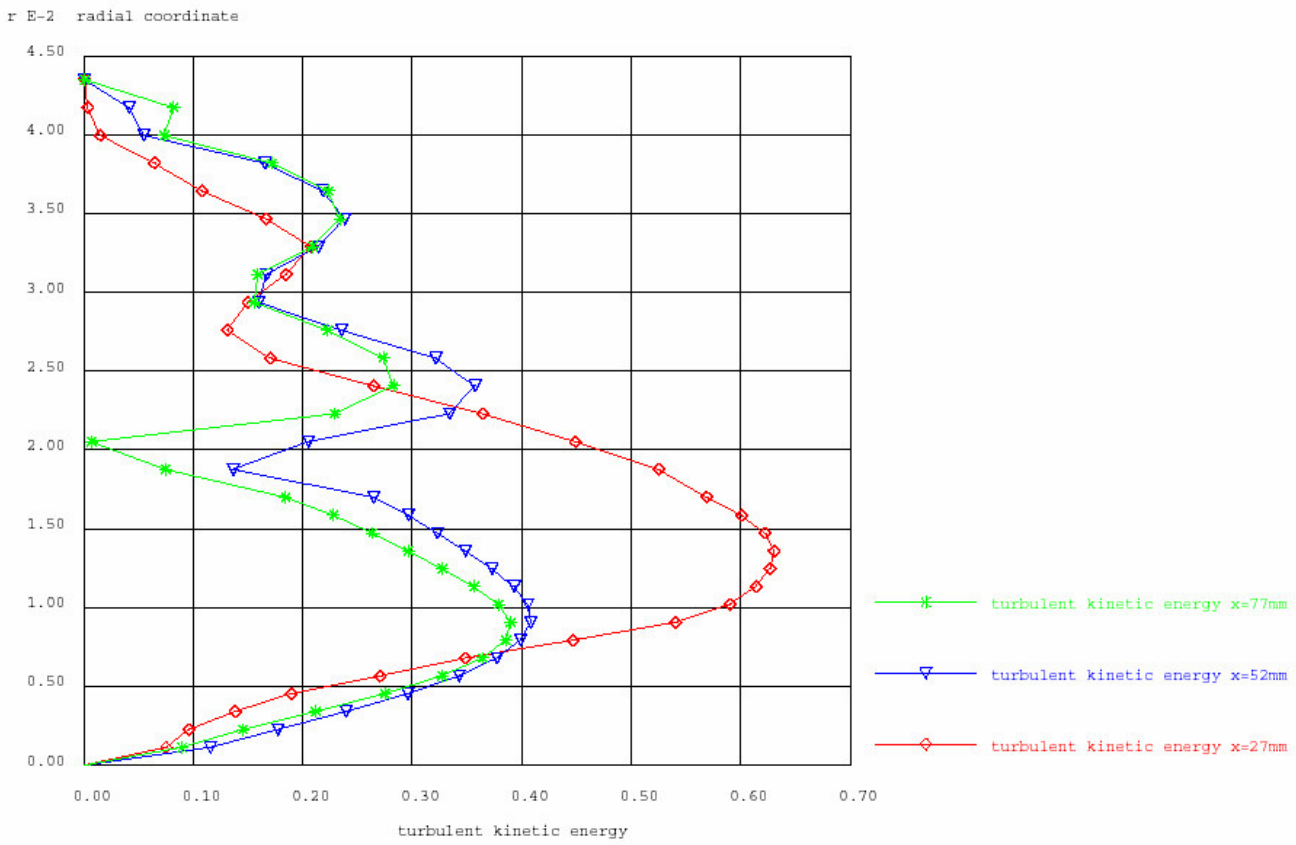

Figure 5. Turbulent kinetic energy for θ = 180°.

the mean angular velocity of the vortices in the target plane at a certain crank angle which is divided by average crank angle velocity (Huang et al., 2005).

The Figure 6 shows the variation of the tumble ratio T_{ca} with the crank angle θ. The magnitude of T_{ca} increases significantly with the downward motion of the piston. It reaches the maximum when θ is equal to 90°. This can be due to the maximum engine speed N (rpm) at θ = 90°. When the crank angle θ becomes superior to 90° and goes to 180°, the tumble ratio is decreasing and reaching a nil value for θ = 180°.

EFFECT OF THE TURBULENCE MODEL INTO THE PRESSURE AND VELOCITY FIELD

Pressure field

The pressure field is simulated when the crank angle θ (teta) is equal to 90°. We show two figures, the first one plots pressure for a position axial direction x equal to 27 mm. The second figure is drawn for 52 mm x position.

The Figures 7 and 8 assert an excellent resemblance between the two curves, the Prandtl model's curve and the k-ε model's curve in the middle of the combustion room. But, we note in the region near the valve piston that the turbulence models do not coincide. For this reason, we can not confirm an exact turbulence model for all the application and perhaps it is better to consider a model in each zone.

Velocity field

To be sure of the previous results, we plot the velocity fields in both axial positions presented in Figures 9 and 10.

In the Figures (9 and 10), we see a perfect coincidence between the two models. Therefore, the Prandtl and the k-ε models predict correctly the velocity fields. In terms of computing time and complexity of formulation, it is better to consider the Prandtl model as an expression of turbulence.

Conclusion

Through this study, we have proved that the numerical simulation by means of finite element method with the arbitrary Lagrangian Eulerian description gives satisfied

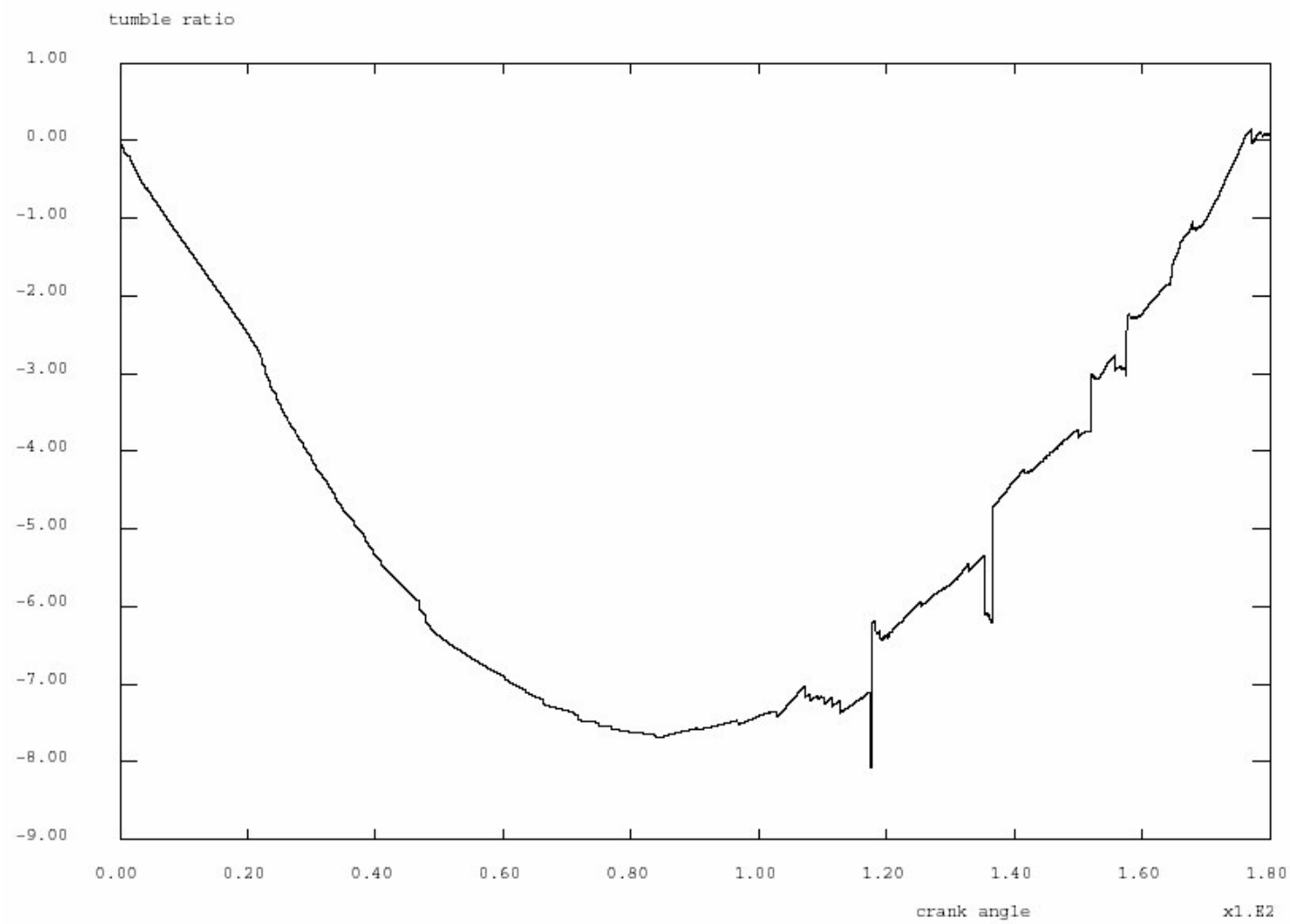

Figure 6. Tumble ratio.

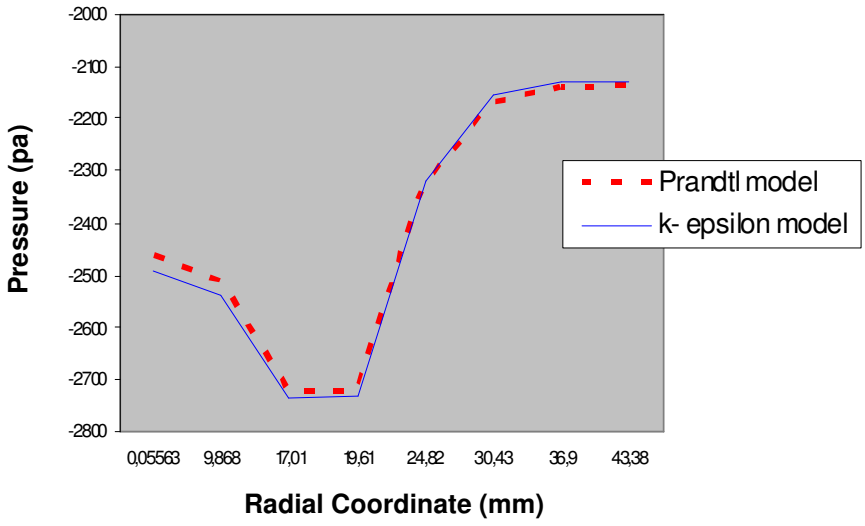

Figure 7. Pressure field (teta = 90°, x = 27 mm).

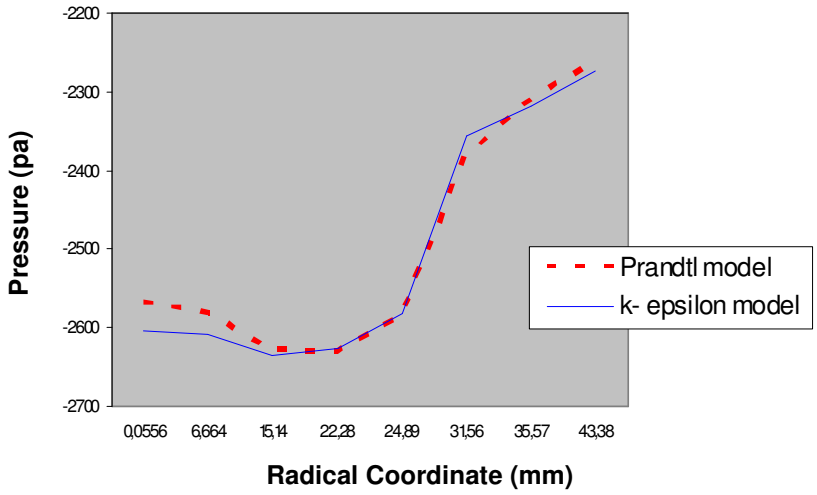

Figure 8. Pressure field (teta = 90°, x = 52 mm).

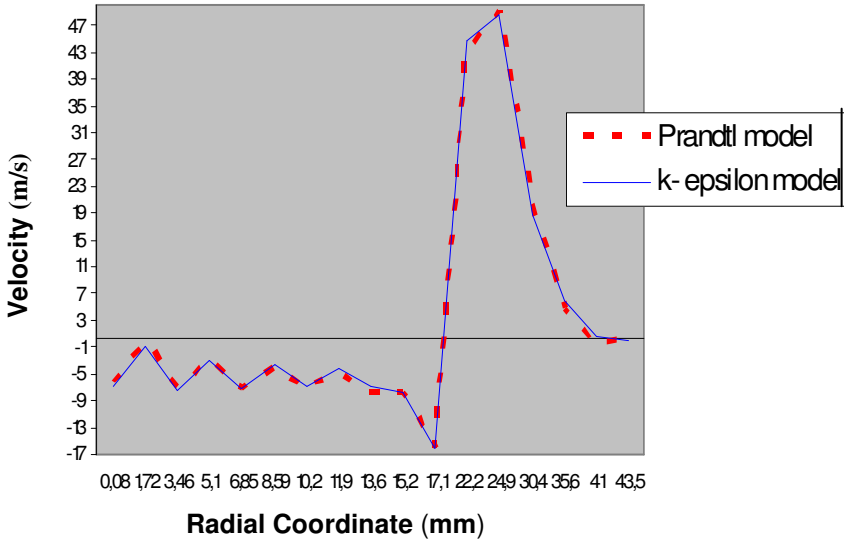

Figure 9. Velocity field (teta = 90°, x = 27 mm).

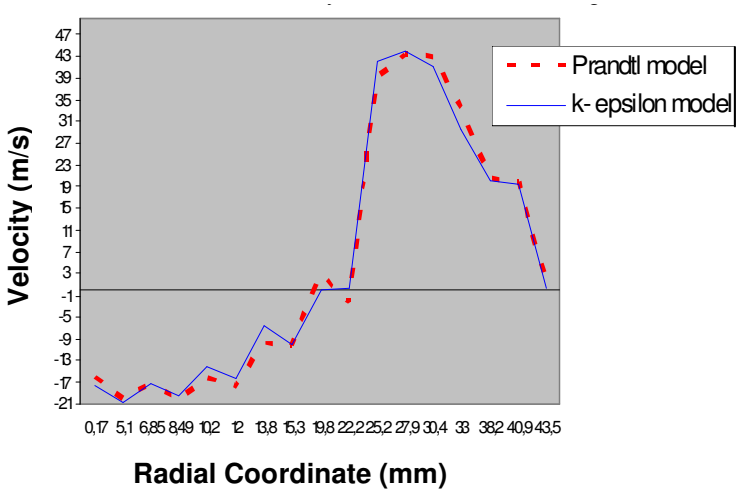

Figure 10. Velocity field (teta = 90°, x = 52 mm).

results compared to the finite volume method. As well, the study of the turbulent kinetic energy conducts to locate the maximum, the minimum and the way of variation from the cylinder symmetry axis to the lateral wall and from the air admission zone to the surface piston. Finally, the tumble ratio drawing has shown a parabolic variation with crank angle interval [0°, 180°]. The peak of magnitude of T_{ca} is obtained at the centre of the mentioned interval corresponding with the maximum engine speed at this crank angle.

Also this study has shown that the Prandtl model can be kept as the turbulence model in predicting the pressure and the velocity fields due to its simplicity and accurate results with regard to the k-ε model.

REFERENCES

Arcoumanis C, Bicen AF, Whitelaw JH (1982). Measurement in a motored four stroke reciprocating model engine. J. Fluids Eng. Vol. 104/235.

Barbouchi Z, Bessrour J(2008). Numerical simulation of aerodynamic and thermal fields inside a cylinder of an alternative engine Int. J. Phys. Sci. 3(3): 079-089.

Boussinesq J (1877). Théorie de l'écoulement tourbillant. Mém. prés. par div. savants a l'académie des Sciences de Paris.

Gazeaux J, Thomas DG (2001). Caractérisation du mouvement de rotation de l'air en écoulement stationnaire dans un monocylindre Diesel en fonction des conditions d'admission. Entropie n° : 234, 13-19.

Gounand S (1997). Simulation numérique d'écoulement à surface libre. CEA/Saclay, Département de mécanique et de technologie, Service d'études mécaniques et thermiques, Rapport DMT.

Haworth DC, Jansen K (2000). Large-eddy simulation on unstructured deforming meshes: towards reciprocating IC engines. Comput. Fluids 29, 493 - 524.

Heywood JB (1987). Fluid motion within the cylinder of internal combustion engines. ASME, J. Fluids Eng. 109: 3-35.

Huang Rf, Huang CW, Yang HS, Lin TW, Hsu WY (2005). Topological flow evolutions in cylinder of motored engine during intake and compression strokes. J. Fluids Struct. 20: 105-127.

Kang KY, Reitz RD (1999). Intake flow structure and swirl generation in a four-valve Diesel engine. Spring Technical Conference, ASME, ICE-vol. 32-2. Paper no. 99-ICE-182.

Kral LD (1998). Recent experience with different turbulence models applied to the calculation of flow over aircraft components. Progr. Aerospace Sci. 34: 481–541.

Launder BE, Spalding DB (1974). The numerical Computation of Turbulent Flows. Comp. Meth. Appl. Mech. Eng. 3: 268-289.

J , Farrel PV (1993). Intake valve flow measurements of an IC engine using particle image velocimetry. SAE paper 930480, Warrendale, PA, USA .

Malcevic I, Ghattas O (2002). Dynamic mesh finite element method for Lagrangian computational fluid dynamics. Finite elements in Anal. Design 38, 965-982.

Prandtl L (1925). Ober Die Ausgebildete Turbulenz ZAMM, 2, 136- 139.

Raghay S, Hakim A (1997). Simulation numérique d'un écoulement dans un moteur alternatif. Entropie n° 206, 33-42.

Snauwaert P, Sierens R (1986). Experimental study of the swirl motion in direct injection Diesel engines under steady state flow conditions. SAE 860026.

Souli M, Zolesio JP (2001). Arbitrary Lagrangian-Eulerian and free surface methods in fluid mechanics. Comput. Meth Appl.Mech.Eng.191, 451-466.

Tippelmann G (1977). A new method of investigation of swirl ports", SAE 770404.

Yun JE (2002). New evaluation indices for bulk motion of in-cylinder flow trough intake port system in cylinder head. J. Automobile Eng. 216: 13- 21.